Inositol 1,4,5-trisphosphate receptors: Immunohistochemical localization to discrete areas of rat brain

ARTICLE *in* NEUROSCIENCE · MAY 1993

Impact Factor: 3.36 · DOI: 10.1016/0306-4522(93)90478-X · Source: PubMed

6 AUTHORS, INCLUDING:

Ted M Dawson
Johns Hopkins University
457 PUBLICATIONS **54,464** CITATIONS
SEE PROFILE

Majid Fotuhi
Johns Hopkins Medicine
33 PUBLICATIONS **4,395** CITATIONS
SEE PROFILE

Neuroscience Vol. 53, No. 4, pp. 927–942, 1993
Printed in Great Britain

0306-4522/93 $6.00 + 0.00
Pergamon Press Ltd

INOSITOL 1,4,5-TRISPHOSPHATE RECEPTORS: IMMUNOHISTOCHEMICAL LOCALIZATION TO DISCRETE AREAS OF RAT CENTRAL NERVOUS SYSTEM

A. H. SHARP,* T. M. DAWSON,*† C. A. ROSS,*§ M. FOTUHI,* R. J. MOUREY*‡ and S. H. SNYDER*‡§‖

The Johns Hopkins University School of Medicine, Departments of *Neuroscience, †Neurology, ‡Pharmacology and Molecular Sciences, and §Psychiatry, 725 N. Wolfe Street, Baltimore, MD 21205, U.S.A.

Abstract—The second messenger inositol 1,4,5-trisphosphate triggers the release of intracellular Ca^{2+} stores upon binding to the inositol 1,4,5-trisphosphate receptor protein, a calcium channel that has been purified and molecularly cloned. To clarify the roles of inositol 1,4,5-trisphosphate receptor in the central nervous system, we have examined in detail the distribution of inositol 1,4,5-trisphosphate receptors in the rat brain and spinal cord using immunohistochemical methods. Inositol 1,4,5-trisphosphate receptors are present in neuronal cells, fibers and terminals in a wide distribution of areas throughout the central nervous system. These include a number of areas not previously reported, such as the olfactory bulb, thalamic nuclei and dorsal horn of the spinal cord. In addition, we have noted a strikingly high density of inositol 1,4,5-trisphosphate receptors in circumventricular organs and neuroendocrine structures such as the area postrema, choroid plexus, subcommisural organ, pineal gland and pituitary.

The distribution of inositol 1,4,5-trisphosphate receptors in discrete structures throughout the central nervous system, including interconnected neuronal systems and neuroendocrine and circumventricular organ structures, presumably reflects the importance of Ca^{2+} release mediated by the phosphoinositide second messenger system in control of diverse physiological processes.

Inositol 1,4,5-trisphosphate ($InsP_3$) derives from the phosphoinositide second messenger system and triggers the release of intracellular calcium (Ca^{2+}) following binding to its receptor protein. The $InsP_3$ receptor ($InsP_3R$) has been purified[35] as a protein of *c.* 1,000,000 mol. wt, comprising four identical subunits which have been molecularly cloned in mouse,[8] rat[18,19] and human.[29] Reconstitution of the $InsP_3R$ in liposomes demonstrates that the protein comprises the Ca^{2+} channel as well as the $InsP_3$ recognition site.[7]

Initial studies by autoradiography revealed discrete localizations of $InsP_3$ in the brain, with extremely high densities in Purkinje cells of the cerebellum and substantial levels in the hippocampus, as well as other areas.[39,40] The limitations of autoradiography precluded localization at a cellular level. Intracellular localizations of $InsP_3R$ at the electron microscopic level in Purkinje cells of the cerebellum reveal a concentration in subcomponents of the endoplasmic reticulum.[19,30,31] In T-lymphocytes, $InsP_3$ influence Ca^{2+} conductance in plasma membrane,[9] while biochemical and immunohistochemical evidence indicates a localization of $InsP_3R$ protein to the plasma membrane of these cells.[15] In olfactory cilia immunohistochemical studies localize $InsP_3R$ to plasma membrane.[28] To clarify the types of synaptic interactions that influence the $InsP_3R$ system, it would be desirable to localize neurons, cells and fibers enriched for $InsP_3R$ by immunohistochemistry at the light microscopic level. Localizations to neuronal processes and terminals are evident in photoreceptor and bipolar cells of the retina.[24] Very recently, limited immunohistochemical mapping for $InsP_3R$ has been reported in developing and adult mouse brain.[22] In the present study we report a detailed immunohistochemical mapping of $InsP_3R$ in rat brain, showing an association of the receptor with cells, fibers and terminals in a number of discrete areas, as well as unique localizations to structures of the circumventricular organ system.

‖To whom correspondence should be addressed.

Abbreviations: BSA, bovine serum albumin; EDTA, ethylenediamine tetra-acetate; $InsP_3$, inositol 1,4,5-trisphosphate; $InsP_3R$, inositol 1,4,5-trisphosphate receptor; NGS, normal goat serum; NRS, normal rabbit serum; PBS, phosphate-buffered saline; SDS–PAGE, sodium dodecyl sulfate–polyacrylamide gel electrophoresis; TBS, Tris-buffered saline.

EXPERIMENTAL PROCEDURES

Purification of inositol 1,4,5-trisphosphate receptor

$InsP_3R$, used for affinity purification of anti-$InsP_3R$ antibodies, for preadsorption controls and for immunization of a goat, was purified to homogeneity from crude rat cerebellar membranes that were solubilized as previously described[7,35] with 1% Triton X-100 or 3-[(3-cholamidopropyl)-dimethylammonio]-1-propane sulfonate. $InsP_3R$ was then purified using heparin–agarose affinity chromatography as described,[7,35] followed by affinity chromatography on $InsP_3$–agarose.[26] Fractions from the heparin–agarose column containing $InsP_3R$ were diluted to an NaCl concentration below 250 mM and incubated batchwise with $InsP_3$–agarose for 30 min. The $InsP_3$–agarose was then poured into a column and washed with 0.1%

Triton X-100 and 250 mM NaCl in homogenization buffer and then eluted with 1 mM phytic acid ($InsP_6$; Sigma) in the same solution. All steps were carried out at 4°C.

Preparation of affinity-purified antibodies

Antibodies against $InsP_3R$ purified from rat cerebellum were raised in New Zealand White rabbits (Harlan Sprague–Dawley, Indianapolis, IN) as previously described.[24] Antibodies were also produced in a goat (mixed Toggenberg/Neubein, Cocalico Biologicals, Reamstown, PA). The goat was initially immunized (day 0) with 500 μg purified $InsP_3R$ in Freund's complete adjuvant by s.c. injection in the inguinal and axillary regions. The goat was subsequently boosted by i.m. injection in the hindquarters and s.c. injection at multiple sites on the back with 250 μg $InsP_3R$ in Freund's incomplete adjuvant on days 14, 21, 35, 60 and 88 following the initial injection. The goat was bled on days 67, 74, 81 and 98, and serum was prepared and stored at −20°C until use. To decrease the concentration of interfering antibodies present in the serum before affinity purification of specific anti-$InsP_3R$ antibodies, crude antiserum from rabbit or goat was adsorbed by sequential overnight batch incubations at 4°C with two affinity matrices. The first consisted of *c.* 20 mg protein extracted from crude brain membranes using high pH (NaOH extract) according to Jay *et al.*[13] and immobilized on CNBr-activated Sepharose. After incubation of the serum with this material, the serum was collected and incubated with the second adsorption matrix, which consisted of solubilized cerebellar membrane extracts that had been treated with heparin agarose (i.e. with the $InsP_3R$ already removed) and immobilized on CNBr-activated Sepharose.[24] Anti-$InsP_3R$ antibodies were purified from the treated serum using purified $InsP_3R$ immobilized on CNBr-activated Sepharose ($InsP_3R$–Sepharose). Approximately 1 mg of $InsP_3R$ was immobilized on 7 ml of resin. The antiserum was incubated batchwise with $InsP_3R$–Sepharose overnight at 4°C. The $InsP_3R$–Sepharose was then poured into a column and washed extensively with 1% Triton X-100 in Tris-buffered saline (TBS; 50 mM Tris–HCl, pH 7.4, 1.5%NaCl) followed by TBS alone. Specific antibodies were then eluted using 4 M $MgCl_2$. Elution was monitored by reading absorbance

Abbreviations used in the figures

A	anterior lobe of the pituitary
aca	anterior commissure, anterior part
Acb	nucleus accumbens
aci	anterior commissure intrabulbar part
AD	anterior dorsal thalamic nucleus
AO	accessory olfactory tract
AP	area postrema
Aq	cerebral aqueduct
AVDM	anteroventral thalamic nucleus, dorsomedial part
AVVl	anteroventral thalamic nucleus, ventrolateral part
BST	bed nucleus of the stria terminalis
BSTL	bed nucleus of the stria terminalis
CA1–CA4	fields of Ammon's horn
cb	cerebellum
Cg	cingulate cortex
CG	central gray
ChP	choroid plexus
Cl	claustrum
CPu	caudate–putamen
cu	cuneate fasciculus
DC, DCo	dorsal cochlear nucleus
DG	dentate gyrus
DH	dorsal horn
dlf	dorsolateral fasciculus
DM	dorsomedial hypothalamic nucleus, compact part
DR	dorsal raphe
EP	entopeduncular nucleus
EPL	external plexiform layer of the olfactory bulb
Fr	frontal cortex
Gl	glomerular cell layer of the olfactory bulb
GN	trigeminal nerve
GP	globus pallidus
Gr	granule cell layer of the cerebellum
I	intermediate lobe of the pituitary
I–VI	laminae of the cerebral cortex
IC	inferior colliculus
ic	internal capsule
ICj	islands of Calleja
IntA	interpositus cerebellar nucleus, anterior part
IntP	interpositus cerebellar nucleus, posterior part
IO	inferior olive
IP	interpeduncular nucleus
LA	lateral amygdaloid nucleus
LC	locus coeruleus
LD	laterodorsal thalamic nucleus
LDVL	laterodorsal thalamic nucleus, ventrolateral part
LG	lateral geniculate
LM	lateral mammillary nucleus
LMol	lacunosum moleculare layer
LP	lateral posterior thalamic nucleus
LR	lateral reticular nucleus
LSI	lateral septal nucleus
MD	mediodorsal thalamic nucleus
ME	median eminence
Med	medial fastigial cerebellar nucleus
mfb	medial forebrain bundle
MG	medial geniculate
MM	medial mammillary nucleus
Mol	molecular layer of the cerebellum
Mtr	mitral cell layer of the olfactory bulb
OB	olfactory bulb
Oc	occipital cortex
opt	optic chiasm
Or	oriens of the hippocampus
P	posterior lobe of the pituitary
PA	preabsorbed antibody
Par	parietal cortex
PDT	posterodorsal tegmental nucleus
Pi	pineal gland
Pir	piriform cortex
Pk	Purkinje cells of the cerebellum
Pn	pontine nuclei
Py	stratum pyramidal of the hippocampus
Rad	stratum radiatum of the hippocampus
SC	superior colliculus
SCO	subcommisural organ
SFO	subfornical organ
SG	substantia gelantinosa
sm	stria medullari
SNc	substantia nigra compacta
SNr, SNR	substantia nigra reticulata
SO	supraoptic hypothalamic nucleus
Sol	solitary tract nucleus
Sp5	spinal tract of the trigeminal nerve
SUM	supramammilliary nucleus
Te	temporal cortex
Tu	olfactory tubercle
VCA	ventral cochlear nucleus
VH	ventral horn of the spinal cord
VL	ventrolateral thalamic nuclei
VP	ventral pallidum
VTA	ventral tegmental area
ZI	zona incerta
3V	third ventricle
5N	trigeminal nucleus
12	hypoglossal nerve

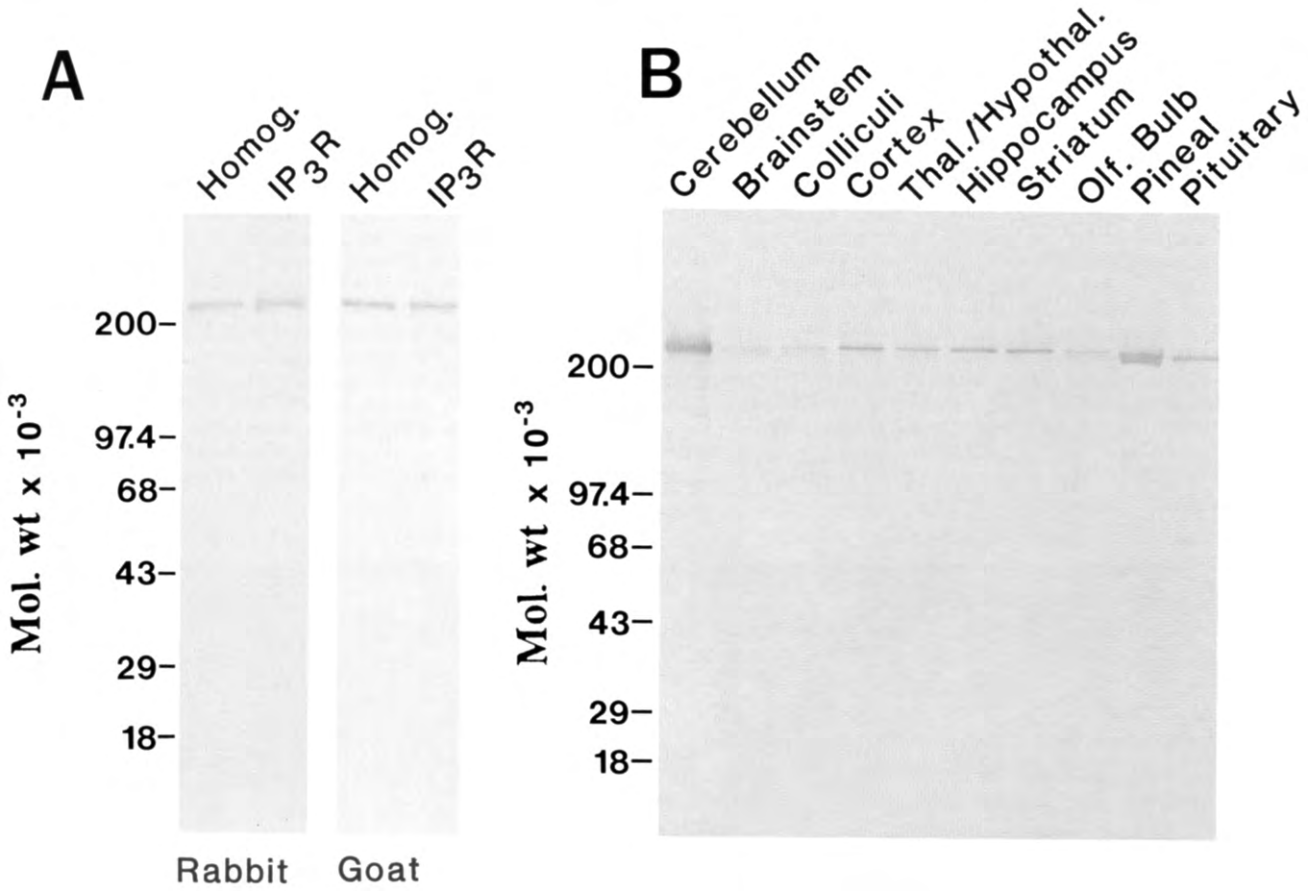

Fig. 1. Immunoblot characterization of affinity-purified anti-$InsP_3R$ antibodies and distribution of immunoreactivity in rat brain. (A) A crude homogenate of rat cerebellum (Homog.; 25 μg) or purified $InsP_3R$ (IP_3R; 1 μg) was subjected to SDS–PAGE and transferred to polyvinylidine difluoride membranes. The blots were then stained with affinity-purified anti-$InsP_3R$ antibodies from rabbit (left; 1:1000 dilution) or goat (right; 1:2000 dilution) as described in Experimental Procedures. (B) Crude membranes were prepared from various regions of rat brain and pineal and pituitary glands, as described in Experimental Procedures. The membrane proteins were resolved by SDS–PAGE (50 μg/lane) and transferred to polyvinylidine difluoride membranes. The blots were then stained with affinity-purified rabbit anti-$InsP_3R$ antibodies (1:1000 dilution), as described in Experimental Procedures. The relative molecular masses of the molecular weight markers ($M_r \times 10^{-3}$) were as follows: myosin, 200; phosphorylase b, 97.4; BSA, 68, ovalbumin, 43, carbonic anhydrase, 29; beta-lactoglobulin, 18.

at 280 nm, and fractions containing protein were pooled and dialysed against 10 mM sodium phosphate (pH 7.4), 150 mM NaCl, 1 mM EDTA and 0.05% NaN_3 for 3–4 h followed by dialysis against two to three changes of 20% sucrose in the same buffer. The affinity-purified antibodies were aliquoted and stored at −70°C until use. Affinity-purified antibodies were used in all experiments.

Preparation of membranes

Male Sprague–Dawley rats (Harlan Sprague–Dawley, Indianapolis, IN) were decapitated, and tissue was rapidly removed and homogenized with a Polytron (Brinkmann) in 8–10 vols of 50 mM Tris–HCl (pH 7.4), 1 mM EDTA, 1 mM 2-mercaptoethanol, 0.4 mM phenylmethylsulfonyl fluoride, 4.8 μg/ml antipain, 9.6 mg/ml leupeptin, 9.6 mg/ml aprotinin, 5 μg/ml chymostatin and 5 μg/ml pepstatin A (homogenization buffer). Homogenization and all subsequent steps were carried out at 4°C. Homogenates were centrifuged for 20 min at 40,000 *g* and the supernatants discarded. Pellets were resuspended in the same buffer and assayed for protein using the Coomassie Blue assay from Pierce.

Sodium dodecyl sulfate electrophoresis and immunoblot analysis

Protein samples were subjected to sodium dodecyl sulfate–polyacrylamide gel electrophoresis (SDS–PAGE) on 1.5-mm-thick 4–16% gradient gels using the system of Laemmli[16] and the separated proteins were transferred to Immobilon-P membranes (Millipore) according to Towbin *et al.*[37] Blots were blocked with 3% bovine serum albumin (BSA) in TBS for 1 h before overnight incubation with affinity-purified antibodies in 3% BSA in TBS. After this incubation, blots were washed three times for 10 min each in 3% BSA in TBS and then incubated with horseradish peroxidase-linked goat anti-rabbit secondary antibody (1:1500 dilution; Boehringer Mannheim) for 1 h at room temperature in the same solution. After three washes of 10 min each in TBS, the blots were developed using H_2O_2 and 4-chloro-1-naphthol as the substrates.

Preparation of tissue and immunocytochemistry

Rats were deeply anesthetized using sodium pentobarbital and perfused with 50 ml of 50 mM sodium phosphate (pH 7.4)–0.9% NaCl (PBS) followed by 200–300 ml freshly

dissolved paraformaldehyde in 100 mM sodium phosphate (pH 7.4). Tissue was then removed by careful dissection and further fixed by incubation in the same solution for 4–18 h. Tissue was then cryoprotected by incubating in 10% sucrose in 100 mM sodium phosphate buffer (pH 7.4) until the tissue sank, followed by sinking in 30% sucrose in the same buffer. Alternatively, tissue was cryoprotected by sinking in 20% glycerol in the same buffer. After freezing the tissue with dry ice, sections (40 μm) were cut into TBS using a sliding microtome. Sections were used fresh or stored at −20°C in an antifreeze solution [10% (w/v) polyvinylprolindone (average mol. wt 40,000), 30% (w/v) sucrose, 10% (v/v) ethylene glycol, 50 mM sodium phosphate, pH 7.4] before use. Sections were permeabilized before immunocytochemistry by incubation in 0.3% Triton X-100 in TBS for 30 min. Sections to be stained with rabbit anti-$InsP_3R$ antibodies were blocked by incubation in 5% normal rabbit serum (NRS) in TBS for 30 min. The sections were then incubated overnight at 4°C with gentle shaking in primary antiserum in 1.5% normal goat serum (NGS) (rabbit antibody) or 1.5% (goat antibody) in TBS containing 0.1% Triton X-100 and 0.05% NaN_3. The affinity-purified anti-$InsP_3R$ antibodies from rabbit or goat were used at a concentration of *c.* 2 μg/ml concentration.

After the primary incubation, the sections were washed three times in TBS for 10 min each. The sections were then incubated with the appropriate biotin-conjugated secondary antibody (goat anti-rabbit or rabbit anti-goat; 1:200 dilution; Vector Laboratories) for 1 h at room temperature in 1.5% normal serum from the same species as the secondary antibody in TBS containing 0.1% Triton X-100. After three washes in TBS, the sections were next incubated with an avidin–biotin–peroxidase complex (Vector Elite, 1:50 dilution; Vector Laboratories) in TBS for 45 min at room temperature. The sections were again washed three times for 10 min each in TBS and were then developed with a substrate solution consisting of 0.1% H_2O_2 and 0.5 mg/ml diaminobenzidine in TBS. Sections were rinsed with TBS and mounted on subbed glass slides. After dehydration, the sections were coverslipped with Permount (Fisher).

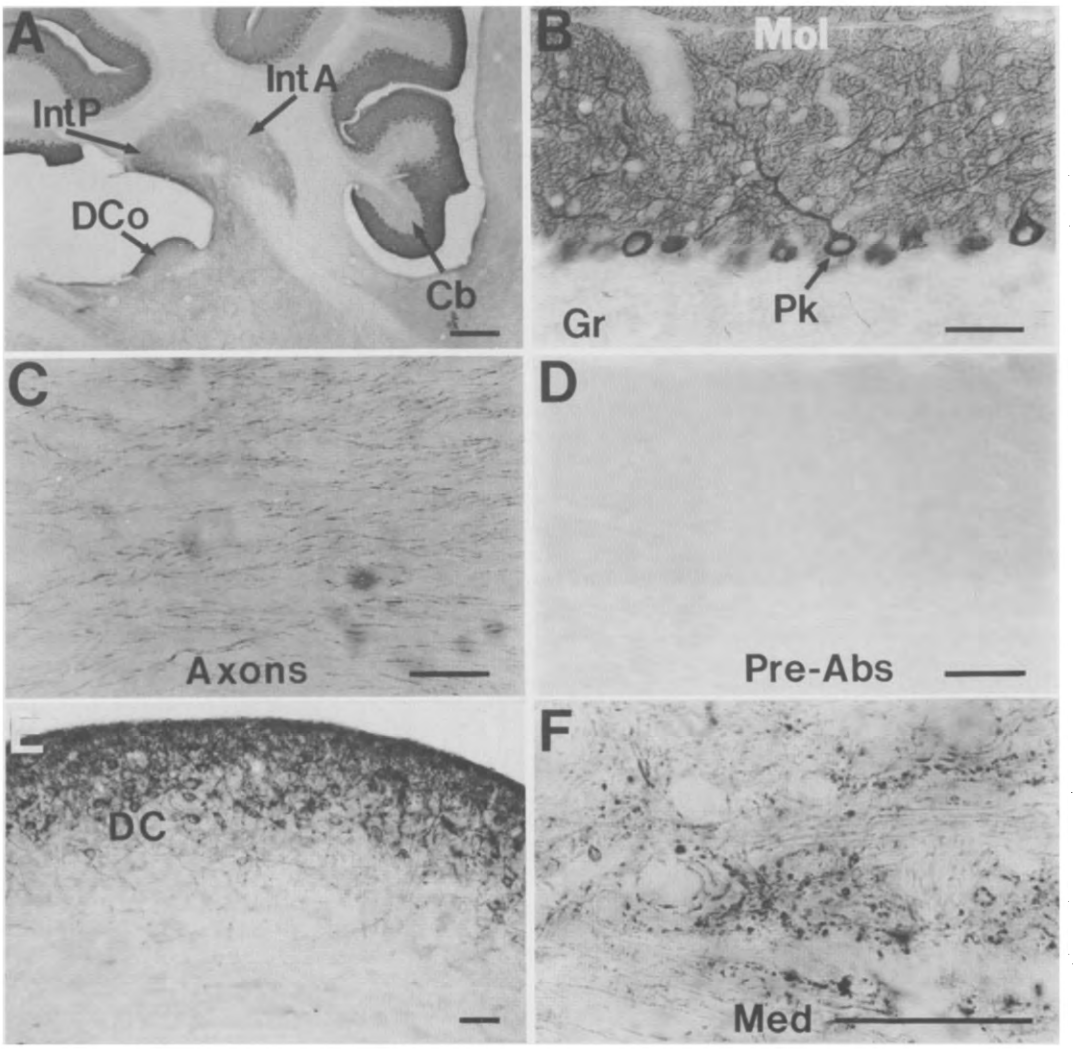

Fig. 2. Distribution of $InsP_3R$ immunoreactivity within the cerebellum and dorsal cochlear nucleus. Note the intense labeling of $InsP_3R$ within the molecular layer of the cerebellum and the immunostaining of Purkinje cell axons (C) which course to innervate deep cerebellar nuclei. Note the absence of staining in D, in which anti-$InsP_3R$ antibodies were preabsorbed with $InsP_3R$ antigen. E Shows the staining pattern of $InsP_3R$ in the dorsal cochlear nuclei. F Shows an example of $InsP_3R$ immunoreactivity in the medial cerebellar nuclei. Note the punctate appearance of staining. Scale bars = 500 μm (A); 50 μm (B–F).

RESULTS

Characterization of immunoreactive inositol 1,4,5-trisphosphate receptor

We used affinity-purified antibodies derived from polyclonal antisera raised in rabbits and goats (Fig. 1). Both antisera display high affinity for $InsP_3R$. Specificity of the antisera is evident in western blots displaying single 260,000 mol. wt bands in rat cerebellar homogenates (Fig. 1A). Western blots demonstrate striking regional variations in $InsP_3R$ densities, as previously reported,[22] with the highest concentration by far in the cerebellum. Strikingly, the pineal gland displays $InsP_3R$ levels higher than any brain region other than the cerebellum. Among the other brain areas, the corpus striatum and cerebral cortex are relatively high, while the olfactory bulb and colliculi are substantially lower. Pituitary $InsP_3R$ densities are lower than pineal but substantially higher than cortex or corpus striatum. All immunohistochemical studies have employed affinity-purified rabbit or goat antisera with identical results obtained with both.

Inositol 1,4,5-trisphosphate receptor localization to cells, fibers and terminals in the cerebellum and dorsal cochlear nucleus

As previously observed,[22,30] the cerebellum at low power displays high densities of $InsP_3R$ in the molecular layer with prominent discrete concentrations in Purkinje cell bodies (Fig. 2). The dorsal cochlear nucleus displays similar high concentrations of $InsP_3R$ as noted previously by Mignery *et al.*[19] (Fig. 2A, E). The interpositus deep cerebellar nucleus stains heavily for $InsP_3R$, with greater intensity in the posterior portion. Cell bodies and processes of Purkinje cells stain prominently (Fig. 2A, B), with no staining evident in sections utilizing antibodies preadsorbed with $InsP_3R$ protein (Fig. 2D). Axons in cerebellar white matter also stain, as do punctate terminals about cells in the lateral and medial deeper cerebellar muclei, as well as the other deep cerebellular nuclei (Fig. 2C, F).

The dorsal cochlear nucleus displays structural homologies to the cerebellum, with the cartwheel cells functionally resembling Purkinje cells.[2,21]

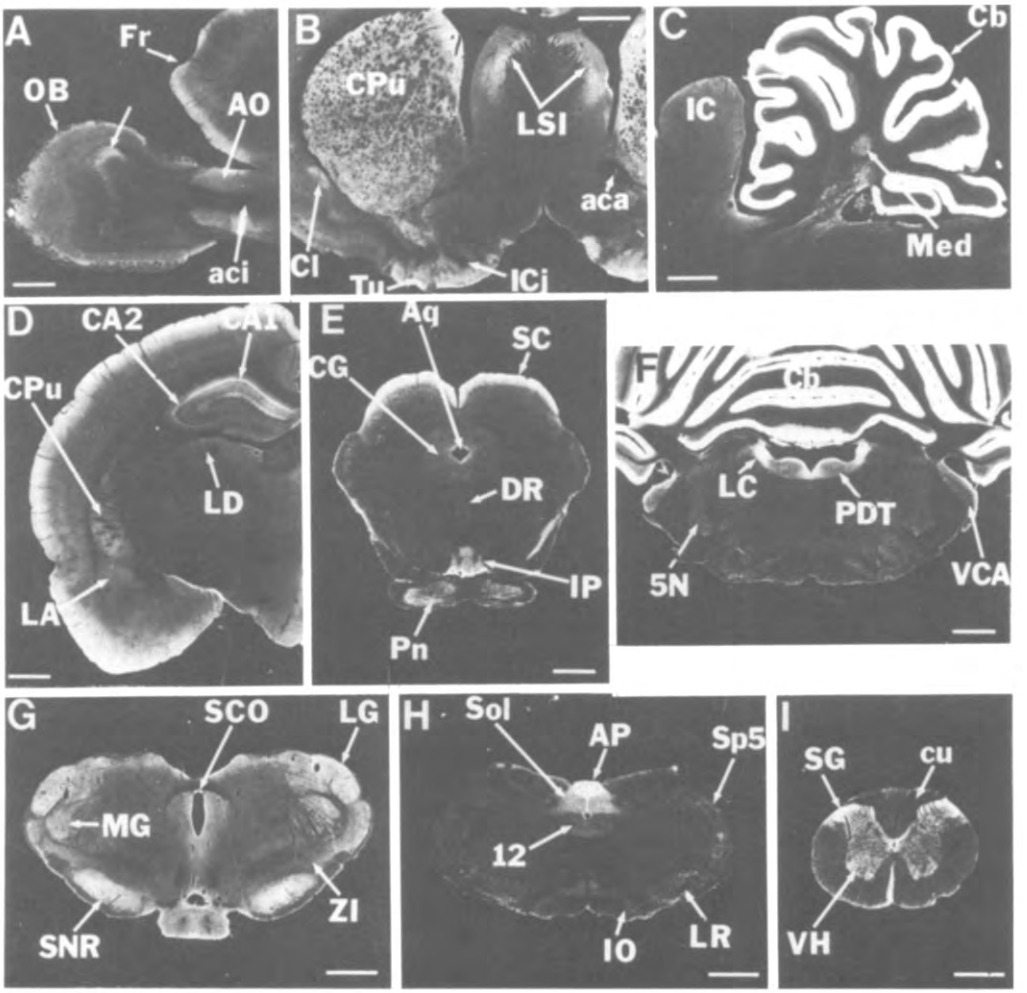

Fig. 3. Low-power dark-field photomicrographs illustrating the overall distribution of $InsP_3R$ immunoreactivity in rat brain. The unlabeled arrow indicates an area which stained non-specifically in the olfactory bulb. Scale bars = 500 μm.

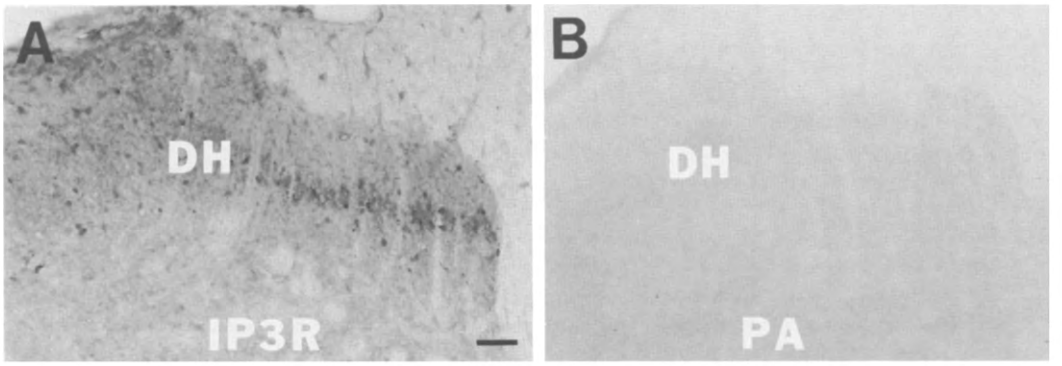

Fig. 4. Bright-field photomicrographs of $InsP_3$ (IP3R) immunoreactivity within the spinal cord. Note the intense staining within the dorsal horn and the absence of staining after preabsorption with $InsP_3R$ antigen. Scale bar = 50 μm.

Interestingly, in the dorsal cochlear nucleus cartwheel cells are intensely stained, comparable to the staining of cerebellar Purkinje cells (Fig. 2E).

Inositol 1,4,5-*trisphosphate receptor in diverse brain regions*

Use of high-affinity antisera has enabled us to detect $InsP_3R$ in a number of discrete areas where it has not been previously observed. For instance, our initial autoradiographic studies[39,40] and recent immunohistochemical investigations[22] failed to detect $InsP_3R$ in the olfactory bulb. We now observe substantial staining in the glomerular layer of the bulb (Fig. 3A) Autoradiographic studies had not identified $InsP_3R$ in the dorsal spinal cord, whereas our immunohistochemical staining reveals high intensities in the substantia gelatinosa with moderate levels in the ventral horn (Figs 3I, 4). Very little characterization of $InsP_3R$ in the brainstem has been reported previously. We demonstrate very intense labeling of $InsP_3R$ in the area postrema and fairly high levels in the closely adjacent nucleus of the solitary tract (Fig. 3H). Other brain stem regions with high concentrations of $InsP_3R$ not previously noted are the locus coeruleus (Fig. 3F), the interpeduncular nucleus (Fig. 3E) and the pontine nuclei (Fig. 3E). As previously observed in autoradiographic investigations,[40] the substantia nigra reticulata has high densities of $InsP_3R$, as do the caudate–putamen, olfactory tubercle and molecular layer of the cerebellum (Fig. 3).

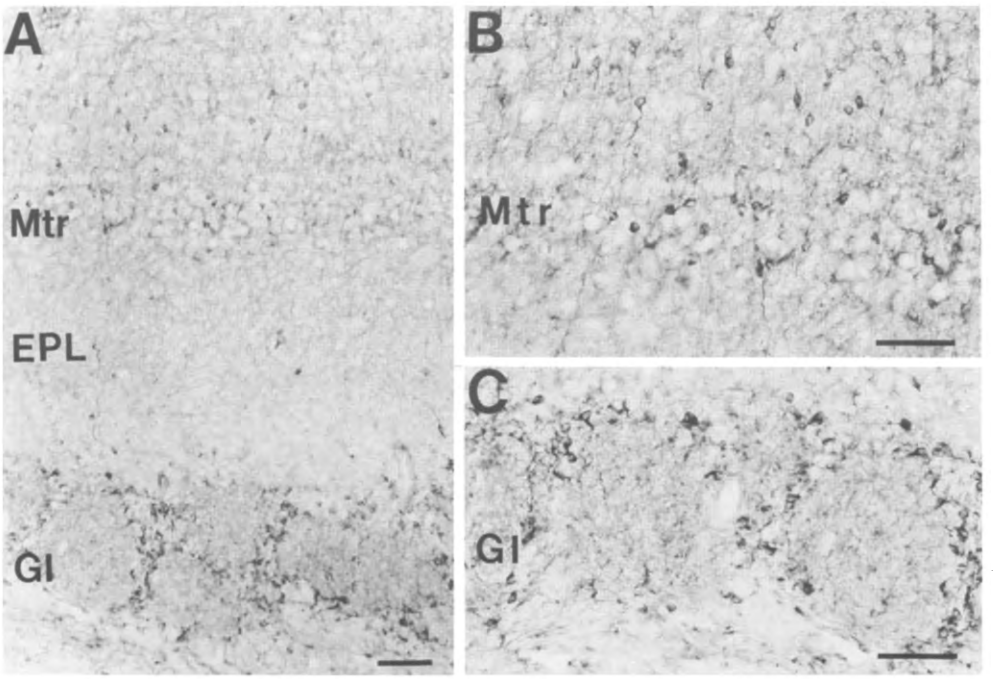

Fig. 5. $InsP_3R$ immunoreactivity within the olfactory bulb. Note the absence of staining within mitral cells (B) and the intense staining of periglomeular cells (C). Scale bars = 50 μm.

Forebrain

$InsP_3R$ densities are discretely localized in the olfactory bulb, and most concentrated in periglomerular cells and their processes (Fig. 5). In the mitral cell layer, $InsP_3R$ occurs in granule cells, while only weak immunoreactivity is occasionally observed in the closely adjacent mitral cells. In the internal granule cell layer, $InsP_3R$ stains intensely in granule cells (Fig. 5).

In the basal ganglia, $InsP_3R$ occurs in substantial densities in the caudate–putamen, nucleus accumbens and olfactory tubercle, with highest concentrations in the olfactory tubercle (Fig. 6). Within the caudate, $InsP_3R$ occurs exclusively in medium spiny neurons and appears to be associated with all such neurons, while very low levels of immunoreactivity are selectively localized in fibers of the adjacent globus pallidus (Fig. 6B). Similarly, in the accumbens, $InsP_3R$ occurs in medium spiny neurons as well as their processes (Fig. 6A). In the ventral tegemental nucleus, which projects to the nucleus accumbens, $InsP_3R$ is highly concentrated in cell bodies of these projection neurons, which are predominantly dopamine containing[6] (Fig. 6D). Similarly, the pars compacta of the substantia nigra displays $InsP_3R$ immunoreactivity in the presumably dopamine-containing cells (Fig. 6C). Very intense staining in neuropil is apparent in the pars reticulata of the nigra (Fig. 6C). The occurrence of $InsP_3R$ in fiber tracts is highlighted by intense staining in fibers of the internal capsule (Fig. 6E).

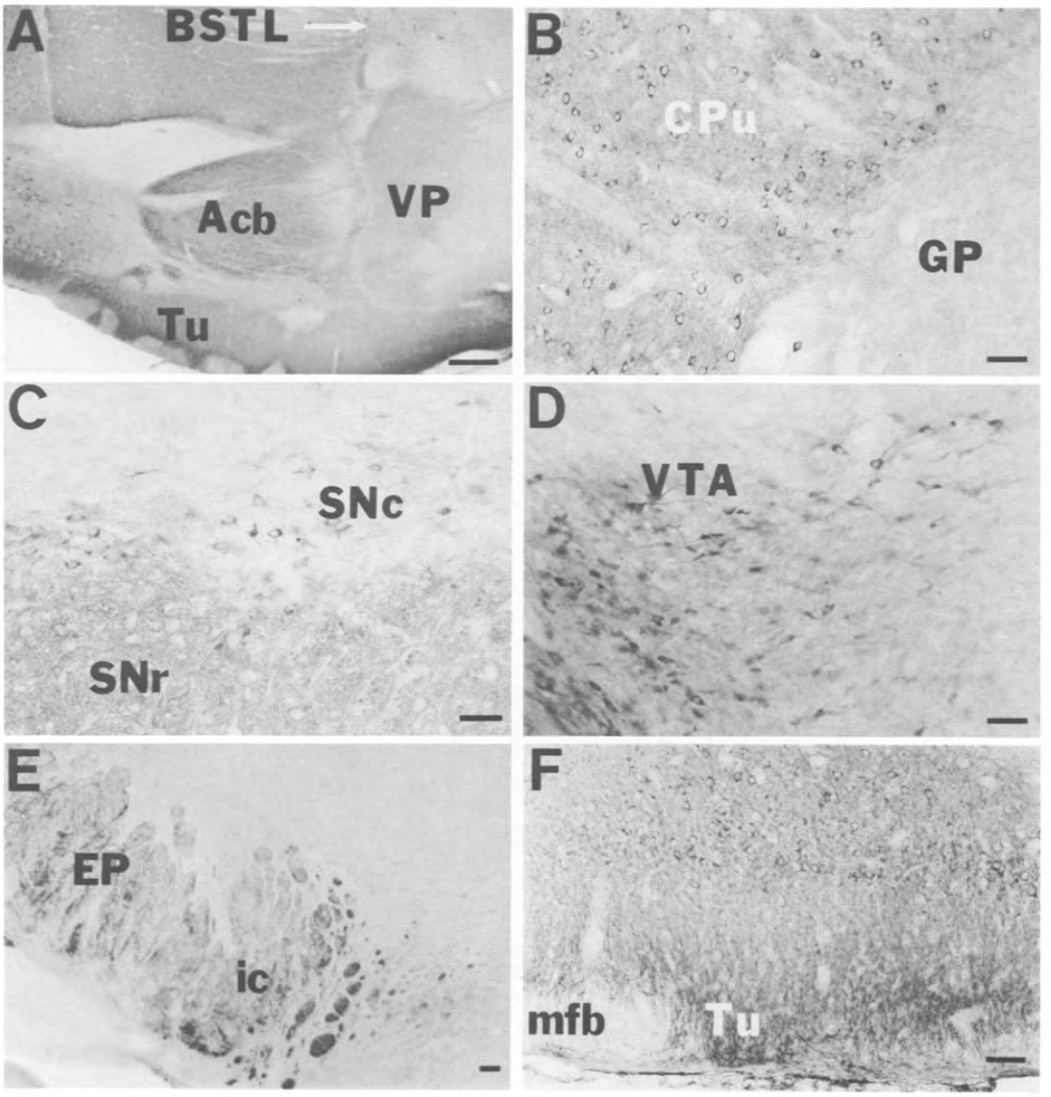

Fig. 6. Photomicrographs of $InsP_3R$ immunoreactivity in the nigrostriatal pathway. In B, note the intense staining of the medium spiny neurons and the moderate staining in the adjacent neuropil. C shows the distribution of $InsP_3R$ in the substantia nigra. Note the cellular staining in the substantia nigra compacta and neuropil staining in the substantia nigra recitulata. E shows $InsP_3R$ immunostaining in the nerve fiber of the internal capsule (ic). Scale bars = 500 μm (A); 50 μm (B–F).

In the cerebral cortex, in the occipital, temporal and parietal areas, intense $InsP_3R$ immunoreactivity is apparent, particularly in cells in layers II, V and VI (Fig. 7). Notable staining is evident in the large pyramidal cells of layer V, as well as the non-pyramidal cells of layer II. The non-pyramidal cells of layer VI in the parietal cortex, which project to the thalamus, also display substantial immunoreactivity. In the cingulate cortex, staining is evident in superficial neuropil and deep cells (Fig. 7C).

In the hippocampus, $InsP_3R$ occurs in numerous structures (Fig. 8). Pyramidal cells are labeled throughout the hippocampus, but most intensely in CA1. Processes of these pyramidal cells are stained in the stratum radiatum and stratum lacunosum-moleculare. Granule cells of the dentate gyrus also stain (Fig. 8E). All areas that project to the hippocampus are rich in $InsP_3R$, specifically cells in the lateral septal nucleus (Fig. 8D), as well as in the entorhinal cortex (data not shown). Terminals of the perforant pathway, which arises from the entorhinal cortex, stain notably for $InsP_3R$ just superficial to stratum lacunosum-moleculaire. Cells in the nucleus of the stria terminalis, which receive prominent projections from the hippocampus, also stain (Fig. 8F).

The mammillary bodies, which receive prominent projections from the hippocampus, display $InsP_3R$ immunoreactivity with high levels in cells in the medial protion of the lateral nucleus, whereas the lateral portion of the lateral nucleus and the medial nuclei are almost devoid (Fig. 9A, B). Fibers coursing into the medial portion of the lateral subdivision are greatly enriched in $InsP_3R$ and could conceivably reflect the hippocampal projections.

Thalamus, hypothalamus and circumventricular organs

Nakanishi *et al.*[22] failed to detect $InsP_3R$ immunoreactivity in the thalamus. We observe

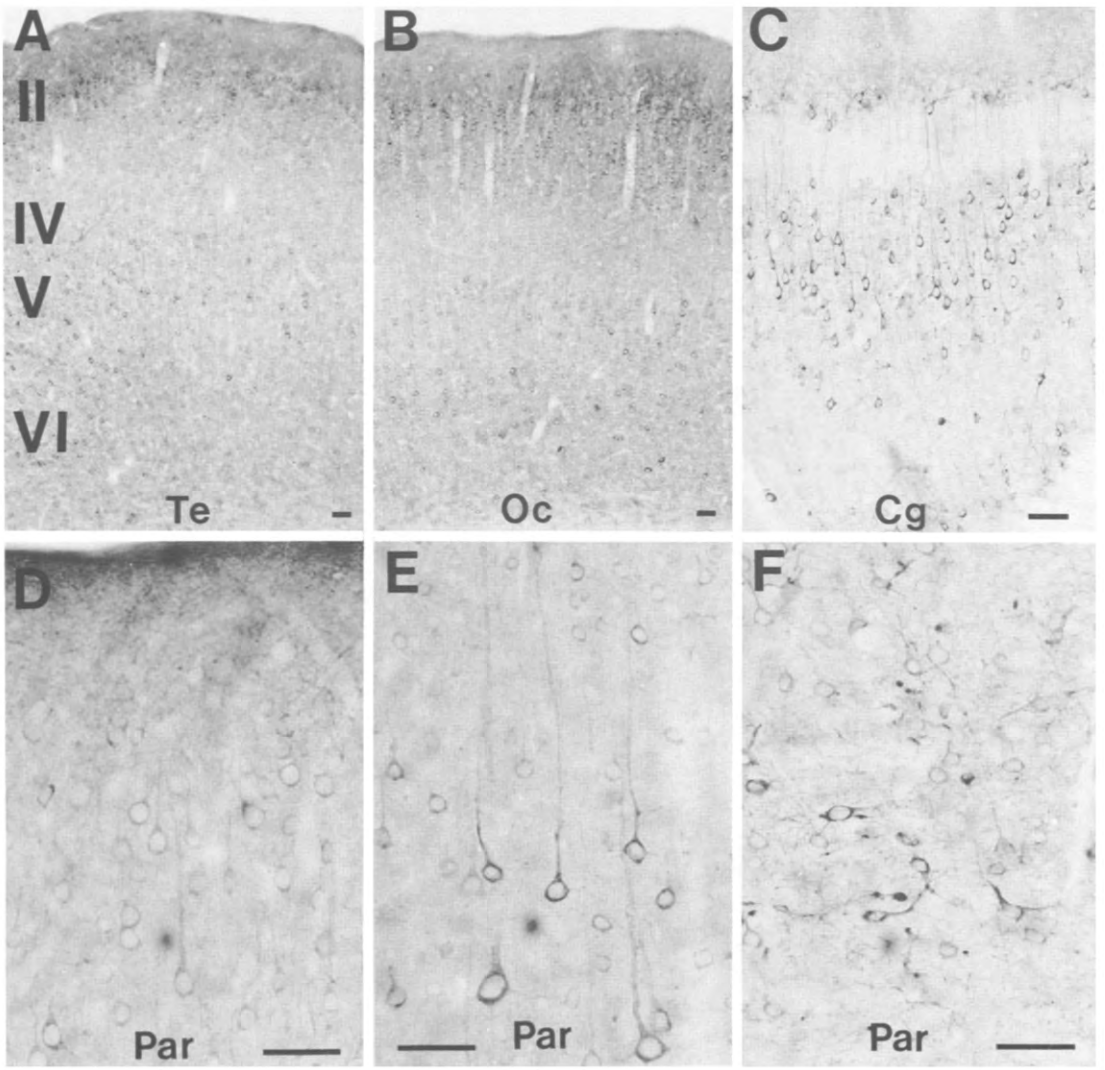

Fig. 7. Distribution of $InsP_3R$ in the cortex of rat brain. Note the intense labeling of pyramidal cells throughout the cortex. Scale bars = 50 μm.

moderate levels of staining in many thalamic nuclei (Fig. 10; Table 1). Typical subnuclei depicted are the ventrolateral and laterodorsal nuclei (Fig. 10B, C), with $InsP_3R$ enriched in cells in the laterodorsal nucleus, with high concentrations of $InsP_3R$ in the larger projection neurons. By contrast, the anterodorsal nucelus of the thalamus displays negligible immunoreactivity and the dorsomedial protion of the anteroventral thalamic nucleus displays only faint immunoreactivity (Fig. 10A).

Some of the most striking $InsP_3R$ localizations in the brain are evident in neuroendocrine structures. In the pituitary, substantial levels are present in discrete cell populations in the anterior lobe, with negligible levels in the intermediate lobe and immunoreactivity occurring in the fiber groups of the posterior pituitary (Fig. 11). The supraoptic nucleus displays $InsP_3R$ in large cell bodies (Fig. 11A), whereas the magnocellular portion of the paraventricular nucleus is essentially devoid of $InsP_3R$. Both supraoptic and paraventricular nuclei project vasopressin neurons to the posterior pituitary, whereas only the supraoptic contains oxytocin cells. The selective association of $InsP_3R$ with cells in the supraoptic nucleus and fibers in the posterior pituitary suggests an association with oxytocin.

The median eminence is enriched in fibers with $InsP_3R$ (Fig. 11B). Cells in the arcuate nucleus, which projects to the median eminence, also contain $InsP_3R$ with highest densities in cells of the ventromedial arcuate and somewhat lesser levels in ventral lateral groups of cells (Fig. 11B). The ventromedial arcuate is rich in somatostatin- and neuropeptide Y-containing neurons, which might reflect those containing $InsP_3R$, whereas the ventral lateral arcuate possesses high densities of growth hormone-releasing factor neurons.[11]

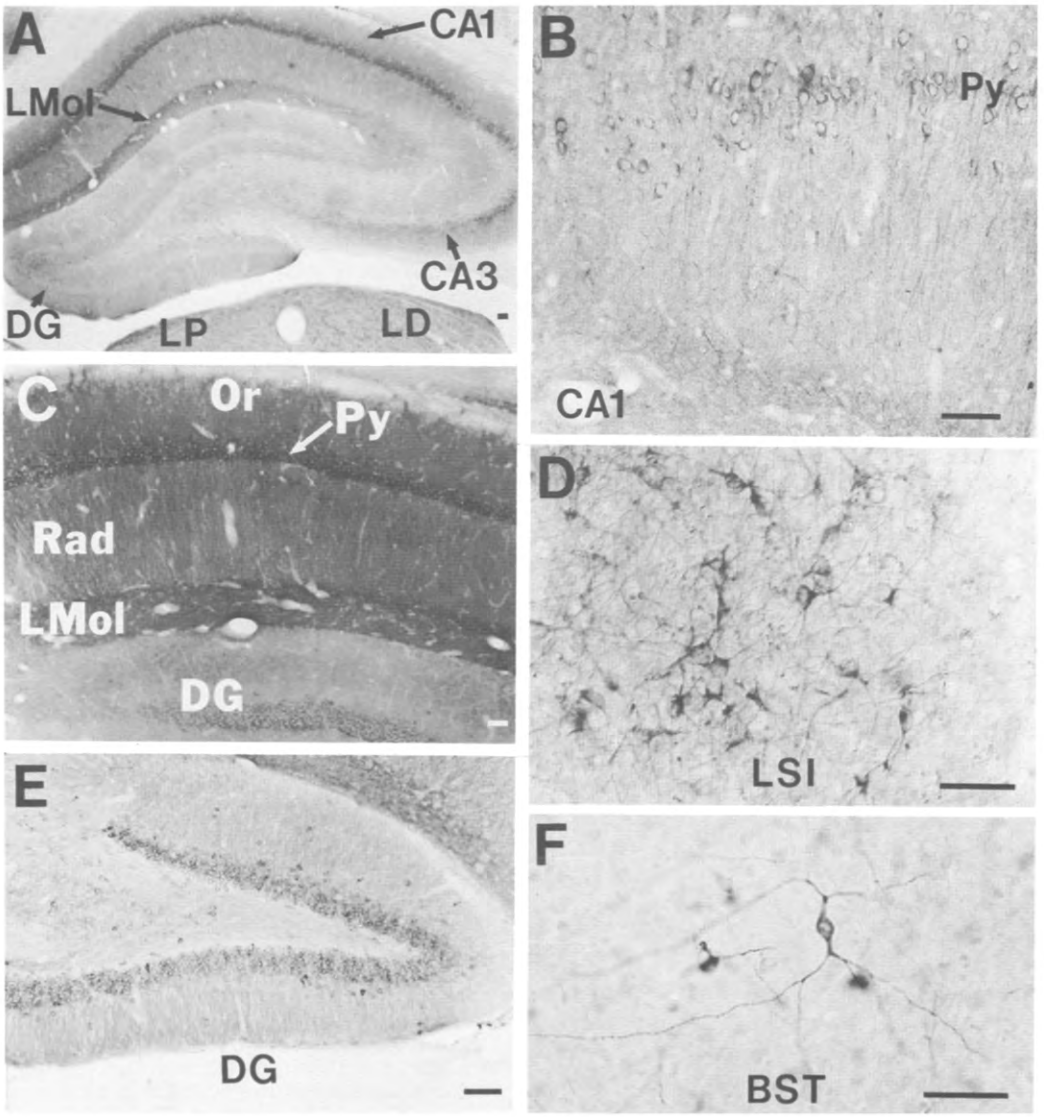

Fig. 8. Bright-field photomicrographs of $InsP_3R$ in the hippocampal pathway. Scale bars = 50 μm.

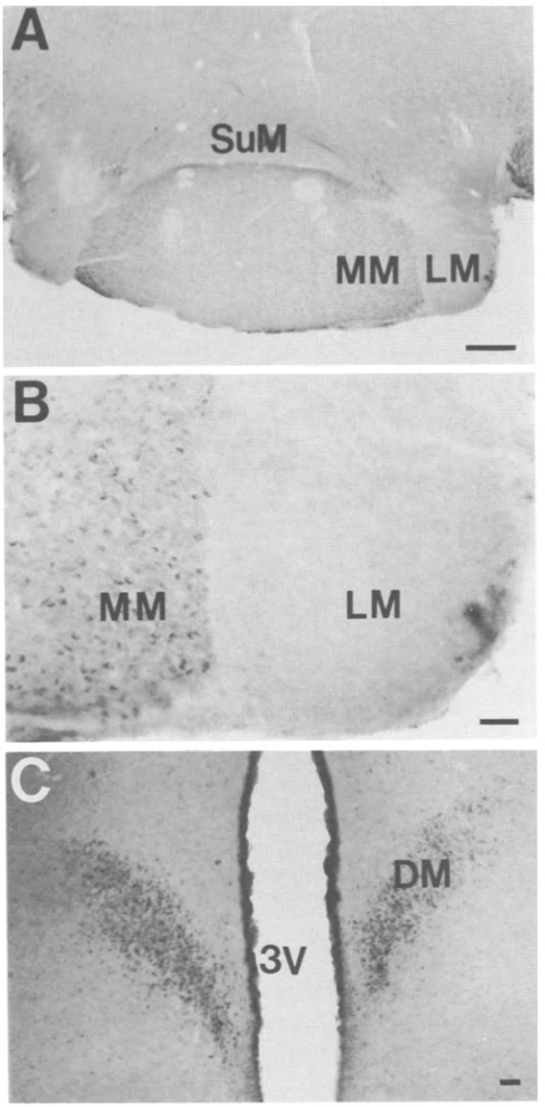

Fig. 9. Distribution of $InsP_3R$ immunoreactivity within the mammillary nuclei and dorsal medial hypothalamic nucleus. Scale bars = 50 μm.

The circumventricular organs are also greatly enriched in $InsP_3R$ (Fig. 12). In the subcommisural organ (Fig. 12A), $InsP_3R$ is concentrated in the ependymal cells, which secrete glycoproteins into the third ventricle.[12] $InsP_3R$ is similarly concentrated in the presumably secretory cells of the choroid plexus. In the subfornical organ, intensely stained $InsP_3R$ fibers are localized at the ventricular surface. The dorsal medial nucleus of the hypothalamus, which projects to the subfornical organ,[36] contains a high density of discretely localized $InsP_3R$ (Fig. 9C). Under low-power (Fig. 3H) and high-power magnification (Fig. 12B), the area postrema displays intense $InsP_3R$ staining cell bodies at the ventricular border with dendrites projecting into the nucleus of the solitary tract.

Extremely high densities of IP_3R are apparent in the pineal gland, with levels about the same as in the nearby molecular layer of the cerebellum (Fig. 12E). Within the pineal gland, IP_3R densities are most evident in pinealocytes (Fig. 12F).

Comparative localizations of inositol 1,4,5-trisphosphate receptor messenger RNA and protein

mRNA occurs only in cell bodies of neurons making a particular protein, while the protein itself can occur throughout the neuron, so that comparing localizations of protein mRNA can shed light on the disposition of the protein being investigated. For instance, in the substantia nigra, the pars reticulata is greatly enriched in $InsP_3R$ protein but displays

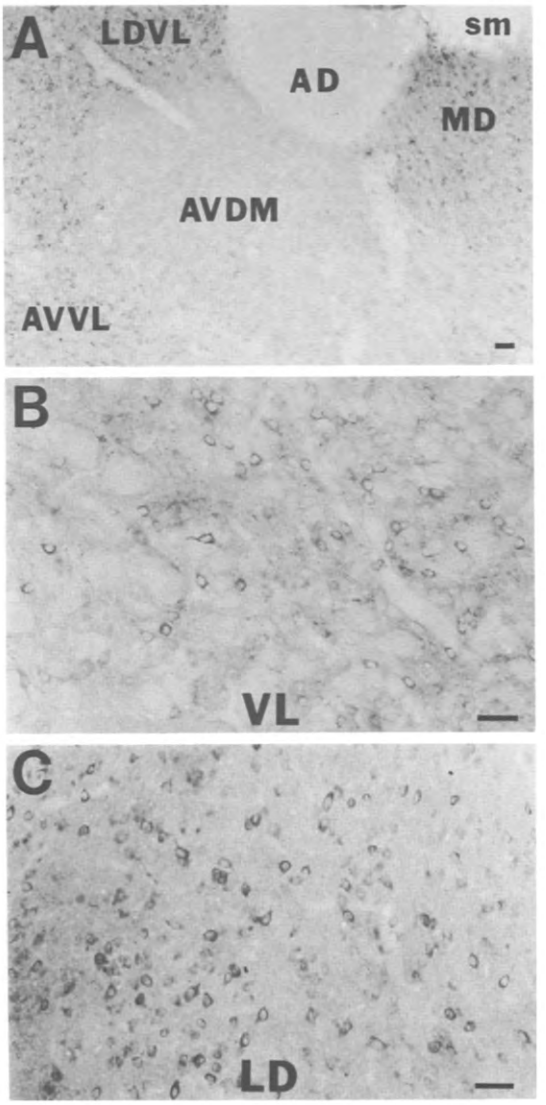

Fig. 10. Bright-field photomicrographs of $InsP_3R$ immunoreactivity within the thalamic nuclei. High-power views of the staining pattern of $InsP_3R$ in the ventrolateral and laterodorsal nuclei are shown in B and C, respectively. Scale bars = 50 μm.

Table 1. Relative densities of inositol 1,4,5-trisphosphate receptor immunoreactivity

Region	Relative density		Region	Relative density	
	Cells	Neuropil		Cells	Neuropil
Olfactory bulb			Hypothalamus		
Olfactory nerve	0	0	Anterior hypothalamic area	1	0
External plexiform layer	1	2	Periventricular nucleus	2	2
Internal granular layer	1	1	Lateral hypothalamic area	0	0
Glomerular layer	2	2	Dorsomedial compact nucleus	3	1
Mitral cell layer	0	1	Ventromedial nucleus	2	1
Anterior olfactory nucleus	3	2	Supraoptic nucleus	3	1
Olfactory tubercle	4	4	Paraventricular nucleus	1	1
Amygdala			Arcuate nucleus	2	2
Lateral nucleus	2	2	Mammillary nucleus	2	1
Basolateral nucleus	3	3	Pituitary		
Basomedial nucleus	3	3	Anterior lobe	4	0
Anterior area	2	2	Posterior lobe	0	2
Central nucleus	3	3	Cerebral cortex		
Medial nucleus	3	3	Neocortex		
Basal ganglia			layer I	0	4
Caudate–putamen	4	4	layers II–VI	3	3
Globus pallidus	0	2	Cingulate cortex		
Accumbens nucleus	4	4	anterior	3	3
Claustrum	4	4	posterior	3	3
Ventral pallidum	0	3	Entorhinal cortex	3	3
Septal area			Piriform cortex	4	4
Lateral septal nucleus	4	3	Cerebellum		
Bed nucleus stria terminalis	3	1	Molecular layer	0	6
Hippocampal formation			Granular layer	1	1
Hippocampus			Deep cerebellar nuclei	0	4
pyramidal cell layer CA1	4	4	Purkinje cell layer	6	—
stratum oriens CA1	0	3	Midbrain		
pyramidal cell layer CA3	2	2	Raphe nucleus	1	0
stratum oriens CA3	0	2	Superior colliculus,		
stratum radiatum CA1	0	3	superficial gray layer	3	2
stratum radiatum CA3	0	1	Central gray	1	1
Dentate gyrus			Red nucleus	0	0
Granular cell layer	2	0	Substantia nigra		
Molecular layer	1	2	compacta	3	2
Hilus	1	0	reticulata	0	3
Subiculum	3	3	Interpeduncular nucleus	3	1
Habenula			Inferior colliculus		
Medial nucleus	0	1	dorsomedial	1	1
Lateral nucleus	0	0	ventrolateral	1	1
Pineal	5	5	Ventral tegmental area	3	2
Thalamus			Pons		
Ventroposterior nucleus,			Pontine nucleus	1	2
lateral and medial	2	1	Locus coeruleus	3	2
Mediodorsal nucleus	2	1	Parabrachial nucleus	1	1
Laterodorsal nucleus	2	1	Medulla oblongata		
Posterior nuclear group	1	1	Nucleus of the solitary tract	1	2
Paratenial nucleus	2	1	Inferior olive	1	1
Reuniens nucleus	1	1	Nucleus of the spinal tract of		
Ventral lateral geniculate nucleus	2	1	the trigeminal nerve	1	1
Dorsal lateral geniculate nucleus	2	1	Spinal tract of the trigeminal nerve	1	1
Medial geniculate nucleus	2	1	Dorsal cochlear nucleus	4	1
Anterior pretectal area	1	0	Ventral cochlear nucleus	1	1
Reticular thalamic nucleus	2	1	Spinal cord		
Rhomboid nucleus	2	1	Substantia gelatinosa	0	3
Gelatinosus nucleus	1	1	Dorsal horn	2	2
Paraventricular nucleus	3	1	Ventral horn	2	2
Parafascicular nucleus	1	1	White matter	1	0
Ventrolateral nucleus	2	1	White matter tracts		
Anterodorsal nucleus	0	0	Corpus callosum	0	1
Anteroventral nucleus			Internal capsule	0	3
Dorsomedial nucleus	1	1	Fornix	0	2
Ventrolateral nucleus	3	1	Anterior commissure	0	0
Anteromedial	3	1	Optic tract	0	0
Zona incerta	0	0	Superior cerebellar peduncle	0	1
Stria medullaris	0	0	Medial lemniscus	0	0

Relative densities of $InsP_3R$ immunoreactivity in various areas of the rat CNS are shown. In this table, the highest density of staining (in cerebellar Purkinje cell and molecular layers) was arbitrarily assigned a value of 6 and the relative densities or other regions were estimated by two independent observers by visual inspection of a large number of representative sections from a total of more than five rats.

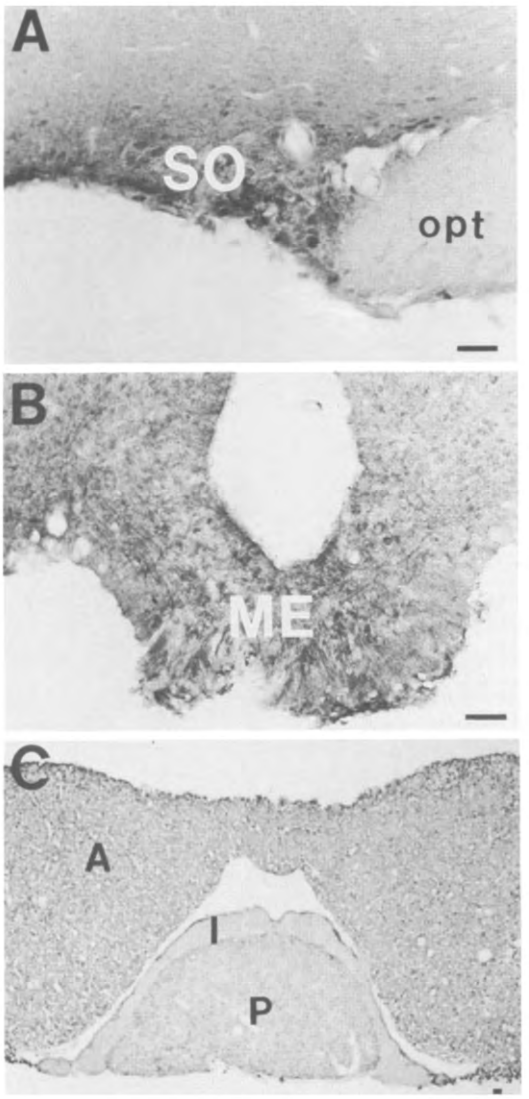

Fig. 11. Distribution of $InsP_3R$ immunoreactivity within the pituitary hypothalamic axis. Scale bars = 50 μm.

negligible mRNA levels by *in situ* hybridization (Fig. 13). This fits with evidence from lesion studies that $InsP_3R$ in the pars reticulata occurs in terminals of the desending striatonigral pathway.[40] By contrast, substantial $InsP_3R$ mRNA is evident in the pars compacta, which contains low levels of immunoreactivity, suggesting that most $InsP_3R$ protein formed by the compacta cells is transported into dendrites or axons.

In the hippocampus, $InsP_3R$ mRNA is evident in pyramidal cells of all layers, with highest levels in CA1. Immunoreactivity also occurs in the pyramidal cells, as well as in the basal and apical dendritic areas. Immunoreactivity lies in a dense band, reflecting terminals of the perforant pathway, consistent with the absence of mRNA in this layer (Fig. 13).

The dentate gyrus contains substantial mRNA in the granule cells, and high levels of $InsP_3R$ immunoreactivity also occur in these cells (Fig. 13). These granule cells project mossy fibers to CA3. Interestingly, no $InsP_3R$ immunoreactivity is evident in the mossy fiber projection area in CA3, suggesting that $InsP_3R$ synthesized in the dentate granule cells functions primarily in the dendrites of these cells, where staining is pronounced.

In the caudate, $InsP_3R$ mRNA is distributed homogeneously, consistent with its occurrence in medium spiny neurons throughout the caudate. The even more homogeneous appearance of immunoreactivity fits with the localization of $InsP_3R$ in fibers as well as cell bodies. In the olfactory tubercle, mRNA is concentrated in cell bodies, whereas $InsP_3R$ protein is evident in more superficial layers corresponding to dendrites of these cells. The endopyriform nucleus and the claustrum contain substantial levels of both $InsP_3R$ and mRNA and protein (Fig. 13).

DISCUSSION

A number of interesting themes are apparent from the diverse localizations of $InsP_3R$. Earlier studies had focused primarily on the concentration of the receptor in endoplasmic reticulum in cell bodies such as Purkinje cells.[19,30,31] Throughout the brain we find high densities of the receptor in neuronal fibers and terminals as well. Earlier we reported high concentrations of $InsP_3R$ in terminals of retinal photoreceptors and bipolar cells.[24] In these sites the phosphoinositide system might be involved in synaptic transmission associated with axo-axonic synapses. Alternatively, nerve terminal depolarization, which triggers calcium influx, might activate the phosphoinositide system to elicit intracellular release of calcium via $InsP_3R$.

A number of interconnected neuronal systems are enriched in $InsP_3R$ and their various components. For instance, most of the neuronal systems of the hippocampus have high densities of $InsP_3R$. Entorhinal neurons enriched in $InsP_3R$ project to granule cells of the dentate gyrus, which contain $InsP_3R$, which in turn project mossy fibers to pyramidal cells of CA3 and CA4 that contain $InsP_3R$, which themselves project Schaffer collaterals to $InsP_3R$-enriched CA1 pyramidal cells.

Particularly striking is the high density of $InsP_3R$ in circumventricular organs and neuroendocrine structures. The choroid plexus and subcommissural organ secrete into the ventricular fluid. The phosphoinositide system has been associated with glandular secretion in the periphery. Indeed, $InsP_3R$ disposition was first characterized in the blowfly salivary gland,[4,5] and extensive studies of $InsP_3R$ release of calcium have been conducted in the lacrimal gland.[3,20] Both exocrine and endocrine pancreas possess robust phosphoinositide systems.[32] In pancreatic beta cells, the phospoinositide system may be involved in insulin release.[23,27] Recently, we have demonstrated $InsP_3R$ localized to endoplasmic reticulum and other

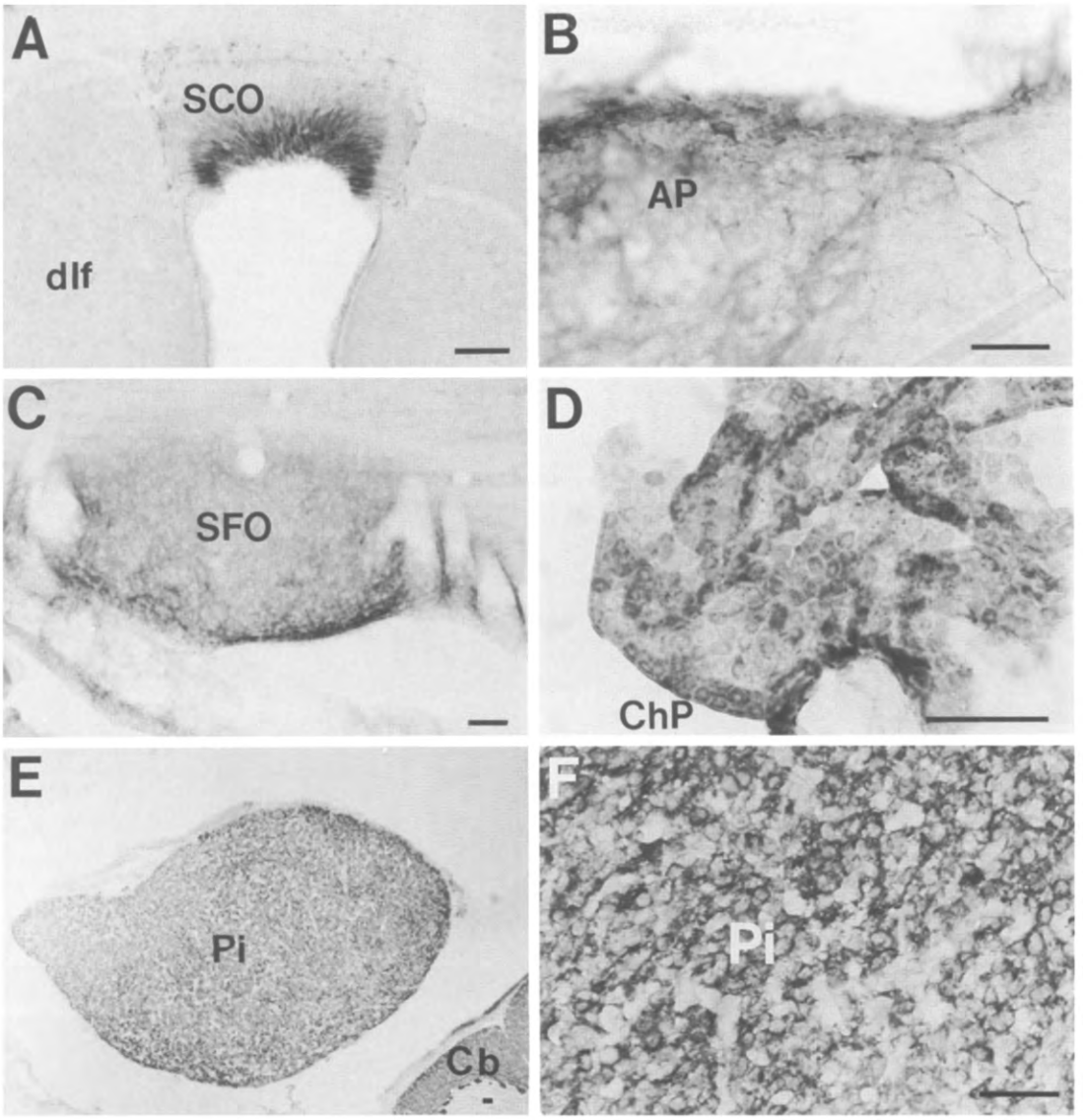

Fig. 12. Photomicrographs of $InsP_3R$ immunoreactivity in circumventricular organs throughout rat brain. Scale bar = 50 μm.

structures of the pancreas.[33] Thus, the $InsP_3R$ may serve a similar role in these circumventricular organs.

High concentrations of $InsP_3R$ in circumventricular organs may reflect substantial densities of receptors associated with the phosphoinositide system. For instance, the choroid plexus and the area postrema are highly enriched in vasopressin V-1 receptors, which act through the phosphoinositide system.[25] Similarly, the subfornical and subcommissural organs and the area postrema are enriched in angiotensin II receptors, which act through the phosphoinositide system.[10,17] The choroid plexus also has high densities of 5-HT_1C serotonin receptors that act by turning on phosphoinositide synthesis.[1] Accordingly, $InsP_3R$ may be involved with signal transduction in these structures.

The exact role of $InsP_3R$ in the pituitary is unclear. The selective localization of $InsP_3R$ in the supraoptic but not the paraventricular nucleus suggests that $InsP_3R$ is contained in oxytocin neurons, but co-localization studies will be required to delineate this possibility. Similarly, we do not yet have direct evidence as to the subtypes of cells in the anterior pituitary that are enriched in $InsP_3R$.

The pineal gland possesses the highest density of $InsP_3R$ of any structures examined except for the cerebellum. The innervation of the pineal gland in the rat derives mainly from sympathetic fibers whose cell bodies are in the superior cervical ganglion.[14] Besides norepinephrine, these neurons also contain neuropeptide Y. The pineal gland is greatly enriched in adenylyl cyclase, as well as both beta and $alpha_1$ adrenoceptors.[34] The extremely high density of

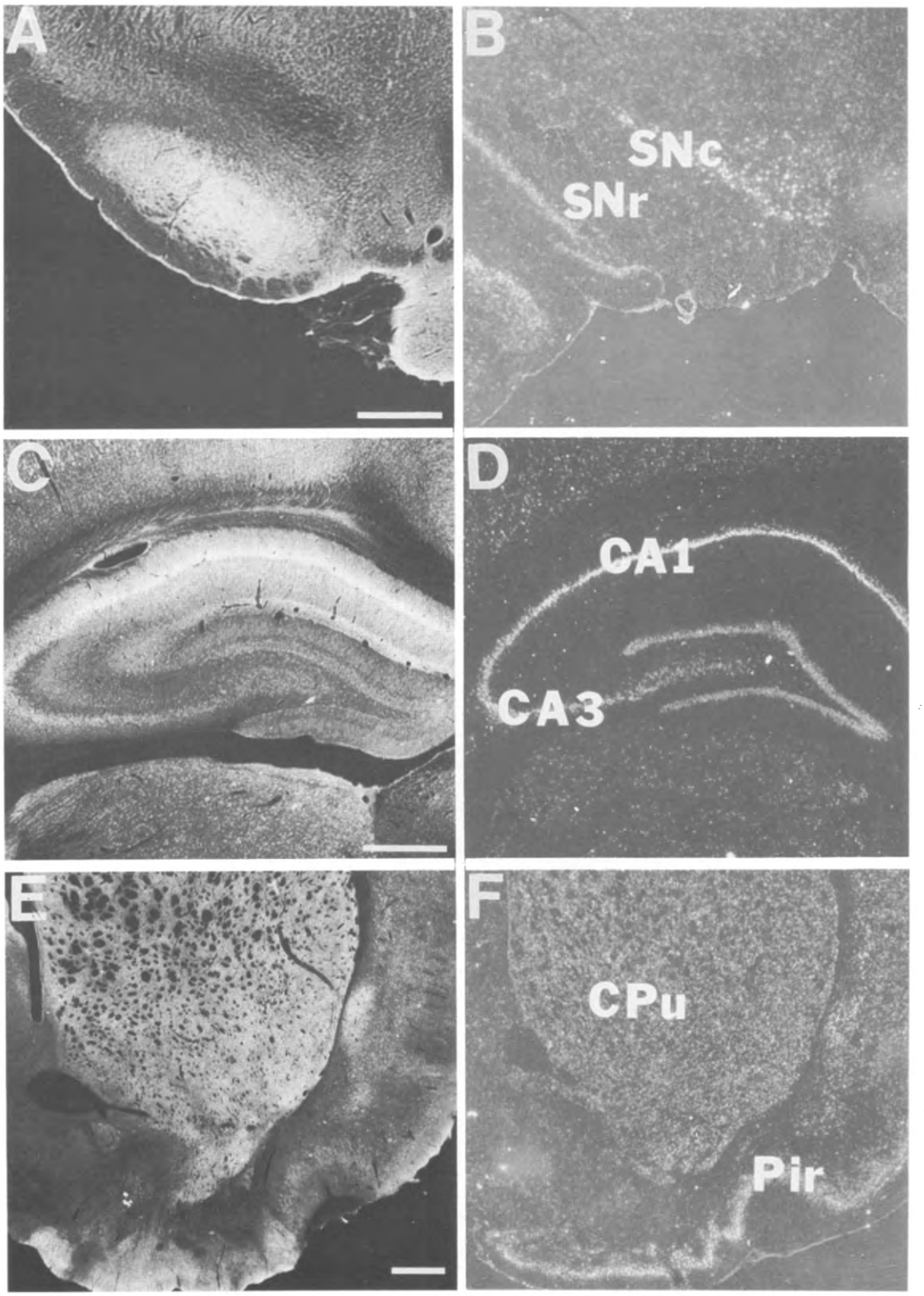

Fig. 13. Comparison between $InsP_3R$ immunoreactivity (A, C and E) and mRNA (B, D and F) within the substantia nigra, hippocampus and striatum. Scale bars = 500 μm.

$InsP_3R$ in ponealocytes suggests that the phosphoinositide system is at least as important in mediating sympathetic regulation of the pineal gland as the cyclic AMP system.

Our results differ in comparison to previous results, mainly in that we detected significant levels of $InsP_3R$ in areas where it was not previously detected; for example, in the thalamus, olfactory bulb and spinal

cord. These differences probably reflect the higher sensitivity or our immunostaining technique, using affinity-purified polyclonal antibodies, in comparison to the previously used autoradiographic detection of bound ligand[39,40] and immunohistochemical staining using monoclonal antibodies.[22] Although $InsP_3$ binds to its receptor with nanomolar affinity, its rate of dissociation is extremely rapid,[41] possibly hampering autoradiographic detection. In comparison to monoclonal antibodies, polyclonal antibodies are typically higher in affinity.

Although $InsP_3R$ has not been previously demonstrated in the spinal cord, our results showing $InsP_3R$ in the dorsal horn are consistent with previous results of physiological studies showing release of intracellular Ca^{2+} in dorsal horn neurons by substance P, a known activator of phosphoinositide turnover.[38]

CONCLUSIONS

$InsP_3R$ immunoreactivity is present in widespread areas of the CNS and is mainly confined to neurons. A number of interconnected neuronal systems are enriched in $InsP_3R$ and immunoreactivity is present in neuronal cell bodies, dendrites, axons and terminals in various areas of the CNS. In addition, strikingly high densities of $InsP_3R$ are present in a number of circumventricular and neuroendocrine structures, including the area postrema, choroid plexus, subcommisural organ, pineal gland and pituitary. These results suggest important roles for the Ca^{2+} release arm of the phosphoinositide second messenger system in control of diverse physiological processes.

Acknowledgements—This work was supported by USPHS grant MH-18501, Research Scientist Aware DA-0074 to S.H.S., training grant GM-07626, grant MH-43040, a NARSAD Young Investigator Award to C.A.R., and a gift from Bristol-Myers Squibb. C.A.R. is a Pew Scholar in the Biomedical Sciences. M.F. is supported by Fonds pour Formation de Checheurs et l'Aide a la Recherche de Quebec. A.H.S. is supported by a Postdoctoral Fellowship from the National Institute of Mental Health, MH-09953. T.M.D. is a Pfizer Postdoctoral Fellow and is supported by grants from the French Foundation, Dana Foundation and the American Academy of Neurology.

REFERENCES

1. Appel N. M., Mitchell W. M., Garlick R. K., Glennon R. A., Teitler M. and DeSouza E. B. (1990) Autoradiographic characterization of (+)-1-(2,5-dimenthoxy-4-[^{125}I]iodophenyl)-2-aminopropane ([^{125}I]DOI) binding to 5-HT2 and 5-HT1C receptors in rat brain. *J. Pharmac. exp. Ther.* **255,** 843–857.
2. Berrebi A. S. and Mugnaini E. (1991) Distribution and targets of the cartwheel cell axon in the dorsal cochlear nucleus of the guinea pig. *Anat. Embryol.* **183,** 427–454.
3. Changya L., Gallacher D. V., Irvine R. F., Potter B. V. L. and Petersen O. H. (1989) Inositol 1,3,4,5-tetrakisphosphate is essential for sustained activation of the Ca^{2+}-dependent K^+ current in single internally perfused mouse lacrimal acinar cells. *J. Membrane Biol.* **109,** 85–93.
4. Fain J. N. and Berridge M. J. (1979) Relationship between hormonal activation of phosphatidylinositol hydrolysis, fluid secretion and calcium flux in the blowfly salivary gland. *Biochem. J.* **178,** 45–58.
5. Fain J. N. and Berridge M. J. (1979) Relationship between phosphatidylinositol synthesis and recovery of 5-hydroxytryptamine-responsive Ca^{2+} flux in blowfly salivary glands. *Biochem. J.* **180,** 655–661.
6. Fallon J. H. and Loughlin S. E. (1985) Substantia nigra. In *The Rat Nervous System* (ed. Paxinos G.), pp. 353–374. Academic Press, Australia.
7. Ferris C. D., Huganir R. L., Supattapone S. and Snyder S. H. (1989) Purified inositol 1,4,5-trisphosphate receptor mediates calcium flux in reconstituted lipid vesicles. *Nature* **342,** 87–89.
8. Furuichi T., Yoshikawa S., Miyawaki A., Wada K., Maeda N. and Mikoshiba K. (1989) Primary structure and functional expression of the inositol 1,4,5-trisphosphate-binding protein P400. *Nature* **342,** 32–38.
9. Gardner P. (1990) Patch clamp studies of lymphocyte activation. *A. Rev. Immun.* **8,** 231–252.
10. Ghiani P., Uva B., Vallarino M., Mandich A. and Masini M. A. (1988) Angiotensin II specific receptors in subcommisural organ. *Neurosci. Lett.* **85,** 212–216.
11. Hökfelt T., Meister B., Villar M. J., Ceccatelli S., Cortes R., Schalling M. and Everitt B. (1989) Hypothalamic neurosecretory systems and their messenger molecules. *Acta physiol. scand.* **136,** 105–111.
12. Ierrera H. and Rodriguez E. M. (1990) Secretory glycoproteins of the rat subcommissural organ are N-linked complex-type glycoproteins. Demonstration by combined use of lectins and specific glycosidases, and by the administration of Tunicamycin. *Histochemistry* **93,** 607–615.
13. Jay S. D., Sharp A. H., Kahl S. D., Vedvick T. S., Harpold M. H. and Campbell K. P. (1991) Structural characterization of the dihydropyridine-sensitive calcium channel α_2 subunit and the associated δ peptides. *J. biol. Chem.* **226,** 3287–3293.
14. Kappers J. A. (1983) Innervation of the vertebrate pineal organ. In *The Pineal Gland and its Endocrine Role* (eds Axelrod J., Fraschini F. and Velo G. P.), pp. 87–112. Plenum Press, New York.
15. Khan A. A., Steiner J. P. and Snyder S. H. (1992) Plasma membrane inositol 1,4,5-trisphosphate receptor of lymphocytes: selective enrichment in sialic acid and unique binding specificity. *Proc. natn. Acad. Sci. U.S.A.* **89,** 2849–2853.
16. Laemmli U. K. (1970) Cleavage of structural proteins during the assembly of the head of bacteriophage T4. *Nature, Lond.* **227,** 680–685.
17. Mendelsohn F. A. O., Quirion R., Saavedra J. M., Aguilera G. and Catt K. J. (1984) Autoradiographic localization of angiotensin II receptors in rat brain. *Proc. natn. Acad. Sci. U.S.A.* **81,** 1575–1579.
18. Mignery G. A., Newton C. L., Archer B. T. III and Sudhof T. C. (1990) Structure and expression of the rat inositol 1,4,5-trisphosphate receptor. *J. biol. Chem.* **265,** 12679–12685.
19. Mignery G. A., Sudhof T. C., Katei K. and DeCamilli P. (1989) Putative receptor for inositol 1,4,5-trisphosphate similar to ryanodine receptor. *Nature* **342,** 192–195.

20. Morris A. P., Gallacher D. V., Irvine R. F. and Petersen O. H. (1987) Synergism of inositol trisphosphate and tetrakisphosphate in activating Ca^{2+}-dependent K^+ channel. *Nature* **330,** 653–655.
21. Mugnaini E. and Morgan J. I. (1987) The neuropeptide cerebellin is a marker for two similar neuronal circuits in rat brain. *Proc. natn. Acad. Sci. U.S.A.* **84,** 8692–8696.
22. Nakanishi S., Naeda N. and Mikoshiba K. (1991) Immunohistochemical localization of an inositol 1,4,5-trisphosphate receptor, P400, in neural tissue: studies in developing and adult mouse brain. *J. Neurosci.* **11,** 2075–2086.
23. Nilsson T., Arkhammar P., Hallberg A., Hellman B. and Berggren P.-O. (1987) Characterization of the inositol 1,4,5-trisphosphate-induced Ca^{2+} release in pancreatic beta-cells. *Biochem. J.* **248,** 329–336.
24. Peng Y.-W., Sharp A. H., Snyder S. H. and Yau K.-W. (1991) Localization of inositol 1,4,5-trisphosphate receptor in synaptic terminals in the vertebrate retina. *Neuron* **6,** 525–531.
25. Phillips P. A., Abrahams M. J., Kelly J., Paxinos G., Grzonka Z., Mendlesohn F. A. O. and Johnston C. I. (1988) Localization of vasopressin binding sites in rat brain *in vitro* autoradiography using a radioiodinated V1 receptor antagonist. *Neuroscience* **27,** 749–761.
26. Prestwich G. D., Marecek J. F., Mourey R. J., Theibert A. B., Ferris C. D., Danoff S. K. and Snyder S. H. (1991) Tethered IP3 synthesis and biochemical applications of the 1-*O*-(3-aminopropyl) ester of inositol 1,4,5-trisphosphate. *J. Am. chem. Soc.* **113,** 1822–1825.
27. Richardson S. B., Eyler N., Twente S., Monaco M., Altszuler N. and Gibson M. (1990) Effects of vasopressin on insulin secretion and inositol phosphate production in a hamster beta cell line (HIT). *Endocrinology* **126,** 1047–1052.
28. Ronnett G. V. and Snyder S. H. (1992) Molecular mechanisms of olfaction. *Trends Neurosci.* **15,** 508–513.
29. Ross C. A., Danoff S. K. Ferris C. D., Donath C., Fischer G. A., Munemitsu S., Snyder S. H. and Ullrich A. (1991) Inositol 1,4,5-trisphosphate receptors (IP3R): cloning of the human cDNA and an IP3R-related mouse cDNA indicating a family of IP3R-related genes. *Soc. Neurosci. Abstr.* **17,** 18.
30. Ross C. A., Meldolesi J., Milner T. A., Satoh T., Supattapone S. and Snyder S. H. (1989) Inositol 1,4,5-trisphosphate receptor localized to endoplasmic reticulum in cerebellar Purkinje neurons. *Nature* **339,** 468–470.
31. Satoh T., Ross C. A., Villa A., Supattapone S., Pozzan T., Snyder S. H. and Meldolesi J. (1990) The inositol 1,4,5-trisphosphate receptor in cerebellar Purkinje cells: quantitative immunogold labeling reveals concentration in an ER subcompartment. *J. Cell Biol.* **111,** 615–624.
32. Sekar M. C. and Hokin L. E. (1986) The role of phosphoinositides in signal transduction. *J. Membrane Biol.* **89,** 193–210.
33. Sharp A. H., Snyder S. H. and Nigam S. K. (1992) Inositol 1,4,5-trisphosphate receptors: intracellular localization in pancreas. *J. biol. Chem.* **267,** 7444–7449.
34. Sugden L. A., Sugden D. and Klein D. C. (1987) $Alpha_1$-adrenoceptor activation elevates cytosolic calcium in rat pinealocytes by increasing net influx. *J. Biol. Chem.* **262,** 741–745.
35. Supattapone S., Worley P. F., Baraban J. M. and Snyder S. H. (1988) Solubilization, purification, and characterization of an inositol trisphosphate receptor. *J. biol. Chem.* **263,** 1530–1534.
36. TerHorst G. J. and Luiten P. G. M. (1986) The projections of the dorsomedial hypothalamic nucleus in the rat. *Brain Res. Bull.* **16,** 231–248.
37. Towbin H., Staehelin T. and Gorden J. (1979) Electrophoretic transfer of proteins from polyacrylamide gels to nitrocellulose sheets: procedure and some applications. *Proc. natn. Acad. Sci. U.S.A.* **76,** 4350–4354.
38. Womack M. D., MacDermott A. B. and Jessell T. M. (1988) Sensory transmitters regulate intracellular calcium in dorsal horn neurons. *Nature* **335,** 744.
39. Worley P. F., Baraban J. M., Colvin J. S. and Snyder S. H. (1987) Inositol trisphosphate receptor localization in brain: variable stoichiometry with protein kinase C. *Nature* **325,** 159–161.
40. Worley P. F., Baraban J. M. and Snyder S. H. (1989) Inositol 1,4,5-trisphosphate receptor binding: autoradiographic localization in rat brain. *J. Neurosci.* **9,** 339–346.
41. Worley P. F., Baraban J. M., Supattapone S., Wilson V. S. and Snyder S. H. (1987) Characterization of inositol trisphosphate receptor binding in brain. Regulation by pH and calcium. *J. biol. Chem.* **262,** 12132–12136.

(*Accepted* 17 *September* 1992)